https://doi.org/10.5194/egusphere-2026-3770
Preprint. Discussion started: 7 July 2026

Regime-dependent reversal in temporal asymmetry of ecosystem carbon exchange across global biomes

Nikhila Gollakota[1], Georgianne Moore[2], Heng Huang[1], Lamberto Rondoni[3,4], Binayak Mohanty[1], and Salvatore Calabrese[1]

[1]Department of Biological and Agricultural Engineering, Texas A&M University, College Station, TX 77843, USA
[2]Department of Biology, Georgia Southern University, 4324 Old Register Road, Statesboro, GA 30460, USA
[3]Dipartimento di Scienze Matematiche, Politecnico di Torino, Corso Duca Degli Abruzzi 24, 10129 Torino, Italy
[4]INFN, Sezione di Torino, Via Pietro Giuria 1, 10125 Torino, Italy

Correspondence: Salvatore Calabrese (salvatore.calabrese@ag.tamu.edu)

Abstract. Terrestrial ecosystems play a central role in regulating the global carbon cycle through exchanges of carbon between land and atmosphere. While ecosystem carbon exchange magnitude has been widely studied, no systematic comparison has examined whether the temporal asymmetry of typical and statistically extreme fluctuations in Net Ecosystem Productivity (NEP) differs across biomes. Here, we quantify the temporal asymmetry of daily NEP trajectories using eddy-covariance observations from 13 FLUXNET sites spanning seven biomes. Specifically, we compare the temporal asymmetry of the top 1 % most extreme NEP fluctuations with that of the full fluctuation distribution to investigate regime-dependent behavior in ecosystem carbon exchange. We find a consistent regime-dependent reversal in temporal asymmetry across all sites and biomes. Extreme NEP fluctuations exhibit positive asymmetry, characterized by a more gradual afternoon decline than morning rise, whereas the full distribution of fluctuations exhibits negative asymmetry, characterized by a steeper afternoon decline than morning rise. Positive asymmetry associated with extreme fluctuations increases with mean air temperature, while negative asymmetry associated with the full fluctuation distribution is most strongly related to vapor pressure deficit. These contrasting relationships indicate a shift in dominant physiological controls, from temperature-regulated photosynthetic capacity during extreme carbon uptake events to VPD-driven stomatal limitation under typical conditions. The consistent reversal in asymmetry observed across diverse ecosystems suggests that diurnal NEP asymmetry is a robust emergent property of ecosystem carbon exchange. Our findings reveal distinct regimes associated with typical and extreme NEP fluctuations and highlight the importance of accounting for regime-dependent ecosystem responses when interpreting and modeling terrestrial carbon dynamics.

1 Introduction

Every year about 14 % of the carbon (C) in the atmosphere is exchanged with the terrestrial biosphere (Lian et al., 2023). This exchange, referred to as Net Ecosystem Productivity (NEP), represents the difference between the C absorbed through photosynthesis (GPP) and the C released through ecosystem (plant and soil) respiration (RECO) and disturbances (DIS) such as fires (Fig. 1a), and is a key indicator of the strength of the ecosystem to act as a C sink, hence to stabilize the Earth's climate (Reichstein et al., 2005; Keenan and Williams, 2018). A fundamental mode of NEP variability is the diurnal cycle (Teng

https://doi.org/10.5194/egusphere-2026-3770
Preprint. Discussion started: 7 July 2026

et al., 2024), generally characterized by a switching from respiration driven fluxes at night (negative NEP) to photosynthesis driven fluxes during the day (positive NEP), with a midday NEP peak whose amplitude varies across ecosystems, climates, and hydrometeorological conditions (Baldocchi, 2008). Critically, the shape of the daily NEP trajectory—how rapidly NEP rises towards its peak and how rapidly it declines afterward—reflects ecosystem functioning, ecosystem carbon exchange dynamics, and underlying ecophysiological controls that cannot be captured by aggregated totals alone (Dietze et al., 2011; Braswell et al., 2005; Wehr et al., 2016). NEP integrates the spatio-temporal dynamics of a myriad of plant and soil microbial species that nonlinearly interact with each other and with multiple abiotic environmental drivers (rainfall, wind, solar radiation, etc.) (Lasslop et al., 2010; Huang et al., 2021; Reitz et al., 2021). This complexity enriches the temporal dynamics of NEP with information about ecosystem functioning, yet it makes it particularly difficult to interpret and predict (Schimel et al., 2019).

Interestingly, the NEP trajectories around the daily peaks are often temporally asymmetric (Li et al., 2005; Xiao et al., 2021; Räsänen et al., 2017), where the asymmetry has been related to the variability of GPP and RECO and the environmental drivers controlling them (Iio et al., 2004; Koyama and Takemoto, 2014; Räsänen et al., 2017). GPP and RECO respond differently to environmental drivers with different sensitivities and on different timescales throughout the day (Lasslop et al., 2010; Braswell et al., 2005; Wehr et al., 2016). Their temporal asymmetry of NEP thus provides an integrated measure that combines the effects of multiple co-varying environmental drivers (radiation, temperature, vapor pressure deficit etc.) on GPP and RECO, capturing how an ecosystem responds to these drivers and relaxes after peak forcing. The extent and direction of asymmetry is thus informative of what dominates the NEP cycle at different times of the day, under different environmental conditions, as well as during typical days vs. days of extremely high carbon uptake, providing insights into possible regime-dependent shifts in ecosystem functioning. For example, shifts between GPP- or RECO-controlled NEP have been observed in diurnal cycles across seasons (Räsänen et al., 2017) or in inter-annual variability across vegetation types (Yuan et al., 2009), with evidence that the coupling between photosynthesis and respiration itself can shift during extreme events (Ping et al., 2023). Yet, to our knowledge no systematic cross-ecosystem analysis has formally quantified how ecosystem function expresses itself in the temporal structure of daily NEP trajectories across biomes across different climates, ecological conditions, and regimes (typical vs. extreme NEP values), and why different asymmetries are observed (e.g., trajectory leading to the peak is steeper than the trajectory leading away from the peak, or viceversa).

Fundamentally, this temporal asymmetry of NEP represents an important emergent property of ecosystem carbon exchange. It reflects the coupled energy, water, and carbon exchanges that underlie land-atmosphere interactions under non-equilibrium conditions that are ultimately driven by solar radiation (i.e., the primary driver of photosynthesis) (Kleidon, 2010, 2016). Capturing this emergent property, especially if there is a shift between typical and extreme conditions, remains a significant challenge because terrestrial biosphere models and machine learning approaches are biased towards typical conditions and mean seasonal cycles, often struggling to accurately estimate short-term temporal anomalies and extreme values (Keenan et al., 2012; Jung et al., 2020). If asymmetry systematically differs during large fluctuations, models developed using typical conditions may not appropriately capture the non-linear interactions that govern extreme carbon exchange (Lemoine, 2021). This further motivates us to investigate temporal NEP asymmetry as an emergent ecosystem property that could shed light on regime-shifts between typical and extreme NEP values.

https://doi.org/10.5194/egusphere-2026-3770
Preprint. Discussion started: 7 July 2026

Analyses of ecosystem carbon exchanges with the atmosphere are complicated by the fact that NEP varies across a range of timescales (Stoy et al., 2005; Baldocchi, 2008). Here we focus on the diurnal scale, where subdaily asymmetry can plausibly arise from the interaction between fast-changing environmental drivers and ecosystem physiological responses. These fluctuations may originate not only from the variability in hydrometeorological drivers (radiation, temperature, wind speed) but also from the response of the ecosystem to these drivers (Stoy et al., 2005; Baldocchi, 2008; Stoy et al., 2009; Vargas et al., 2010). Traditional ecological approaches have advanced our understanding of land–atmosphere carbon dynamics, but they often overlook the regime-dependent variability (Rastetter et al., 2023). In particular, statistical extremes in NEP trajectories, which may carry disproportionate weight in determining ecosystem–climate feedbacks, remain underexplored. Recent work has in fact shown the importance of (low and high) GPP extremes in the C balance and its response to changes in environmental conditions (e.g., warming) (Li et al., 2022). However, methods that can capture regime-dependent shifts in ecosystem functioning are needed.

Quantifying temporal asymmetry requires approaches that explicitly characterize the directional evolution of fluctuations rather than their magnitude alone. Statistical physics provides one such framework through novel statistical physics approaches developed within the context of small—often biological—thermodynamic systems, which have been proving useful for analyzing environmental variability and its impact on system fluctuations (Toussaint and Schneider, 1998; Jørgensen and Svirezhev, 2004; Cochran et al., 2016; Fang et al., 2019; Yin et al., 2024). In particular, the theories for non-equilibrium fluctuations (Evans and Searles, 2002; Evans et al., 2008; Andrieux et al., 2007), describe characteristic asymmetries related to the degree of irreversibility or of entropy production, such as the fluctuation theorem (Evans and Searles, 2002), which quantifies the statistical asymmetry between forward and backward trajectories in non-equilibrium systems (Talkner and Hänggi, 2020; Rondoni, 2021). Within the context of NEP variability these approaches provide effective measures, rooted in the concept of non-equilibrium thermodynamics, to quantify the temporal asymmetry in NEP time-series and investigate how environmental drivers shape these temporal patterns.

Here, we investigate whether diurnal NEP trajectories exhibit a systematic regime-dependent temporal asymmetry across global biomes, whether this asymmetry differs between typical and statistically extreme NEP fluctuations, and which environmental drivers dominate the observed asymmetry in each regime. Guided by the hypothesis that NEP asymmetry and its environmental drivers are regime-dependent, we quantify the temporal asymmetry in NEP trajectories around their daily peak using eddy-covariance time-series from 13 sites spanning seven biomes within the FLUXNET network. In analogy with statistical physics, we refer to any deviation from the long-term mean NEP as a "fluctuation", with no reference to either deterministic or stochastic components. Fluctuations thus include daily cycles and seasonality. Our analysis explicitly distinguishes between the top 1 % statistical extremes (defined as values exceeding the 99^{th} quantile of NEP, without reference to climatic extremes) and full distribution of fluctuations. We then conclude by discussing the universality of the asymmetry across sites, its regime-dependent drivers, and its implications for ecosystem carbon dynamics and modeling.

https://doi.org/10.5194/egusphere-2026-3770
Preprint. Discussion started: 7 July 2026

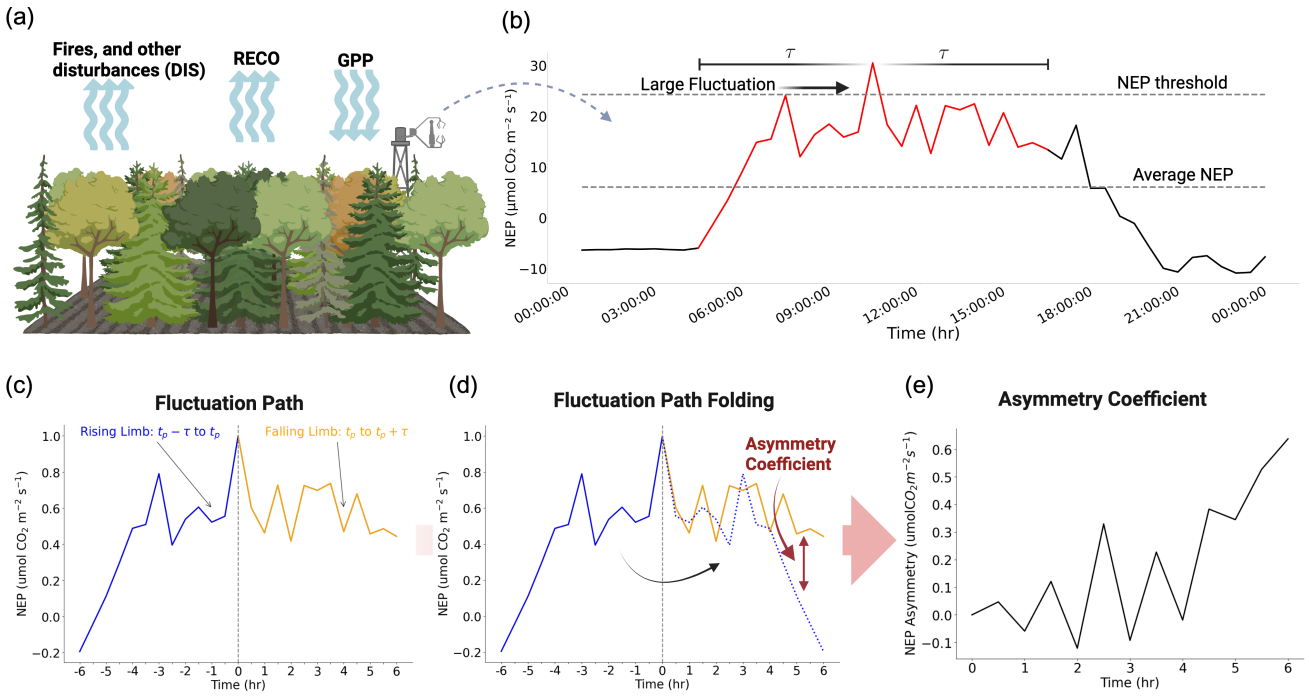

Figure 1. Diagram illustrating the estimation of time-asymmetry in NEP time-series. (a) Schematic of an ecosystem showing the three components of NEP: gross primary production (GPP, carbon uptake via photosynthesis), ecosystem respiration (RECO, carbon release by plants and soil microbes), and disturbances (DIS, e.g., fires), measured by an eddy-covariance tower. (b) Sample half-hourly NEP time-series over one day, showing a large fluctuation (red) that exceeds the NEP threshold and a smaller fluctuation (black) that does not. The dashed lines indicate the NEP threshold and long-term average NEP. The window of width 2τ, centered on the peak timestamp t_p, is indicated. (c) Fluctuation path extracted from the large fluctuation in (b), showing the rising limb (blue, $t_p - \tau$ to t_p) and falling limb (orange, t_p to $t_p + \tau$), with time zero at the peak. (d) Folded fluctuation path showing the rising and falling limbs overlaid about the peak, with the asymmetry coefficient A_t computed as the difference between the falling and rising limbs at each time step t. (e) Asymmetry coefficient profile A_t over time, where positive values indicate a more gradual afternoon decline than morning rise and negative values indicate a steeper afternoon decline than morning rise.

2 Data and methods

2.1 Data and site selection

We considered NEP time-series from 13 different sites, representing various biomes. The characteristics of each site are provided in Table S1 of the supplementary information. These sites are part of FLUXNET, a global network of eddy-covariance sites adhering to the same data processing pipeline and data quality control protocols (Pastorello et al., 2020, 2021). Among the hundreds of sites that are part of FLUXNET2015, we selected sites that met a set of criteria as of June 6$^{\text{th}}$, 2024. First, we excluded wetlands, snow and ice covered sites, and water bodies due to intricate NEP dynamics controlled by water levels or

https://doi.org/10.5194/egusphere-2026-3770
Preprint. Discussion started: 7 July 2026

ice, and cropland, urban and built-up lands due to human-induced disturbances. The remaining ecosystems include: shrubland, grassland, savanna, and three forest types (deciduous broadleaf forest; evergreen broadleaf forest; evergreen needleleaf forest). Second, we excluded sites that do not have at least 3 years of data of Net Ecosystem Exchange (NEE), Soil Water Content, Shortwave Radiation, Gross Primary Production, and Ecosystem Respiration. Third, we only considered sites with continuous soil temperature and soil water content (at least at a depth of 10 cm) data that were gap-filled only with high confidence (MDS quality flag ≤ 1). Fourth, we excluded sites with Mean Annual Temperature (MAT) below 5°C to avoid complications from freeze-thaw events. Finally, for NEP, we used the NEE_VUT_REF product directly, which is the reference Net Ecosystem Exchange estimate produced by the ONEFlux pipeline after friction velocity filtering, gap-filling, and model-efficiency-based selection (Pastorello et al., 2020). No additional quality-control filtering of NEE was applied in this study.

For each site, we extracted half-hourly Net Ecosystem Exchange (NEE), which was converted to NEP (NEP = -NEE), along with meteorological variables including air temperature (T), incoming shortwave radiation (SW), vapor pressure deficit (VPD), and precipitation (P) from FLUXNET gap-filled products (suffix `_F`). We also downloaded ecosystem respiration (RECO) and gross primary production (GPP) from both daytime and nighttime partitioning methods, as well as soil water content (SWC), which was restricted to records with quality flag ≤ 1 (measured or high-quality gap-filled values), along with the ISO timestamp marking the end of each averaging period. Table S2 of the Supplementary Information provides the corresponding FLUXNET variable names and descriptions.

The half-hourly eddy covariance data used for our analysis are processed through a rigorous and standardized quality assurance and quality control (QA/QC) pipeline across all FLUXNET sites (Pastorello et al., 2020). This processing includes spike detection, friction velocity (u^*) filtering to remove data from periods with low turbulence, Marginal Distribution Sampling (MDS) gap-filling, and random uncertainty estimation following the approach of Hollinger and Richardson (2005).

For time-series expressing a net flux of a system property, here NEP, there are multiple possible measures of asymmetry. One could compare the positive and negative tails of the NEP probability distribution to evaluate the skewness of the distribution as a measure of asymmetry, reflecting the tendency of observing more NEP fluctuations in one specific direction (Talkner and Hänggi, 2020). However, this approach—related to the fluctuation theorem (Evans and Searles, 2002)—focuses on the tails of the distribution, neglecting temporal information about the evolution and dynamics of NEP fluctuations, and is not readily generalizable to the entire distribution. Here, we adopted a different approach—directly related to irreversibility in statistical physics (Paneni et al., 2006, 2008; Porporato et al., 2011)—that is based on quantifying the asymmetry in each fluctuation as the temporal asymmetry between its rising and falling limbs. When computed for multiple fluctuations, this asymmetry reflects both the effects of the external force driving the system away from equilibrium and its nonlinear response and tendency to return to equilibrium—the core origin of irreversibility (Caruso et al., 2020; Marconi et al., 2008). This approach based on asymmetry applies directly to net fluxes, i.e., NEP, rather than its partitioned components (GPP and RECO), which could introduce biases based on the chosen partitioning method (Lasslop et al., 2010; Reichstein et al., 2005).

We began by identifying “large" fluctuations, defined as those fluctuations that exceed a threshold (Fig. 1(b)). The threshold was calculated based on a reference NEP value, such as its mean. In this case, the threshold is expressed as

$$\mathrm{NEP}^{\mathrm{threshold}} = \mu + c\sigma, \tag{1}$$

https://doi.org/10.5194/egusphere-2026-3770
Preprint. Discussion started: 7 July 2026

where μ is the mean of the values of NEP for a chosen time period, σ is the standard deviation of NEP, and c is a coefficient that can be adjusted to move the threshold closer or farther from the mean. For each site, the coefficient 'c' was chosen so that the same percentage of fluctuations crosses the threshold. For each of the fluctuations crossing the threshold, we first identified their peak, $\mathrm{NEP}^{\max}$, and their respective peak time, t_p (Fig. 1). After identifying the peak values, we identified the fluctuation paths, namely the path represented by the rising and falling limbs of the fluctuations (Paneni et al., 2008). These can be found based on a meaningfully chosen time window of width 2τ about the peak, $[t_p - \tau; t_p + \tau]$. Considering the daily dynamics of NEP, largely influenced by photosynthetic activity, we selected $\tau = 6$ hours. Thus, for each peak whose absolute value exceeds the chosen threshold, the fluctuation path is the set of values that NEP takes on within a time interval of width 2τ (12 hrs) centered around the peak (Fig. 1). For comparison between sites, we then normalized each fluctuation path by their peak NEP value,

$$\mathrm{NEP}_{\mathrm{t}}^{\mathrm{FP}} = \mathrm{NEP}_{\mathrm{t}}/\mathrm{NEP}^{\max}, \tag{2}$$

where t is a time variable within the fluctuation path with origin at the time of peak t_p ($-\tau \leq t \leq \tau$).

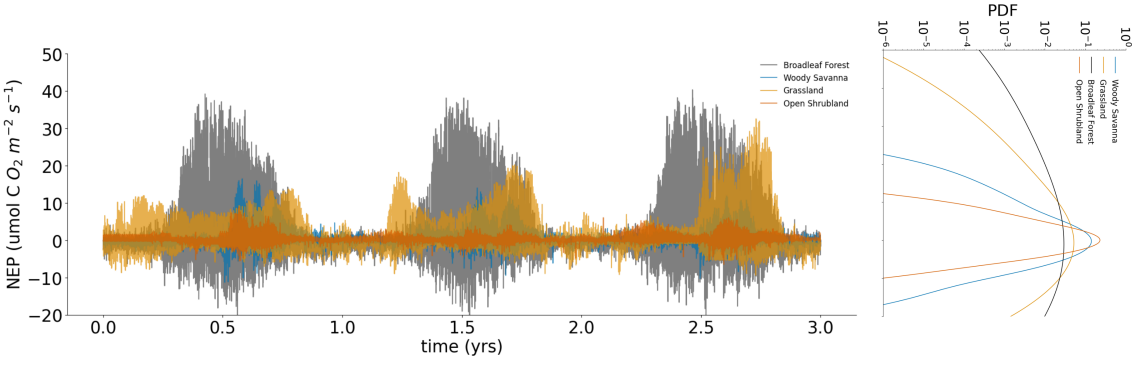

Figure 2. Sample time-series of NEP for four selected sites, presented with half-hourly data frequency and their corresponding probability density functions (PDFs).

Nevertheless, because eddy covariance measurements can be noisy, a potential concern while identifying fluctuation paths is that the timestamp of a peak of an individual fluctuation may be due to random measurement error, instead of a true maximum. The asymmetric metric used here is calculated by averaging all fluctuation paths at each site (Eq. (3)). Therefore, the random errors in individual peak timestamps would be distributed around both positive and negative deviations and tend to cancel out when averaged, thus producing a reliable estimate of the mean asymmetry. This approach of taking the average is consistent with how the same metric was originally applied in statistical physics (Paneni et al., 2006, 2008) as well, where ensemble averaging is the standard means of extracting meaningful asymmetry signals from noisy trajectories.

After having identified and juxtaposed all fluctuations paths, one can observe, statistically, the temporal symmetry/asymmetry (Fig. 1(c)). To quantify the latter, we used an asymmetry coefficient computed from the difference between falling and rising limbs of the fluctuations. Specifically, for each fluctuation path (or directly for the average fluctuation path) we folded the

https://doi.org/10.5194/egusphere-2026-3770
Preprint. Discussion started: 7 July 2026

fluctuation path about its peak and computed for each t between 0 and τ the difference between the two limbs of the fluctuation (Fig. 1(d)),

$$A_t = \mathrm{NEP}_{\mathrm{t}}^{\mathrm{FP}} - \mathrm{NEP}_{-\mathrm{t}}^{\mathrm{FP}} \tag{3}$$

where $\mathrm{NEP}_{\mathrm{t}}^{\mathrm{FP}}$ is the falling limb after the peak and $\mathrm{NEP}_{-\mathrm{t}}^{\mathrm{FP}}$ is the rising limb before the peak. Mainly, we focused on the average of A_t, $\overline{A}_t$, over all fluctuation paths (Paneni et al., 2008),

$$\overline{A}_t = \frac{1}{N}\sum_{i=1}^{N} A_t^i, \tag{4}$$

where we added a superscript i to indicate that it is a sum over all fluctuation paths. This measure of time asymmetry in fluctuations is a direct estimation of thermodynamic irreversibility (Paneni et al., 2008; Porporato et al., 2011), which originates as a statistical difference between forward and backward trajectories. For each fluctuation path, we also analyzed the peak asymmetry value, $\overline{A^{max}}$ (i.e., $\max(A_t)$), which can be positive or negative, depending on the sign of asymmetry. The distribution of peak asymmetry values $A^{\max}$ over all fluctuation paths at each site is also explored to investigate the contribution of individual fluctuation paths to the average asymmetry (e.g., a near zero asymmetry can be obtained by nearly symmetric paths or by paths with contrasting asymmetries that average out).

To investigate how the asymmetry varies between large fluctuations and typical daily fluctuations, we first quantified the asymmetry of large fluctuations, defined as the top 1 % fluctuations, namely the coefficient c was selected such that only 1 % of the fluctuations cross it. Because extreme events are identified based on this statistical threshold, we assessed whether gap-filled values influence their detection by evaluating the NEE_VUT_REF quality control flag for all identified peak timestamps. Across all sites, 87.6 % (2,252 of 2,571) of extreme event peaks correspond to directly measured half-hourly periods (QC = 0), while 12.4 % (319 events) are gap-filled (QC > 0). These gap-filled extremes are distributed across all 13 sites, with no individual site contributing more than 16 % of the total (Table S5). Because the MDS gap-filling algorithm reconstructs missing values from meteorologically similar periods with moderate flux magnitudes (Pastorello et al., 2020), gap-filled values that happen to exceed the extreme threshold represent conservative estimates rather than artifacts, and would therefore attenuate rather than amplify the patterns reported here.

We then compared the asymmetry of the top 1 % fluctuations (extremes) with the one of all daily fluctuations, selected by setting $c = 0$ (threshold becomes equal to the long-term average NEP). To assess the impact of the choice of threshold, we repeated the analysis using the top 2 % (98th quantile) and top 5 % (95th quantile) of NEP fluctuations. The results are shown in Figure S6 of the Supplementary Information. A comprehensive overview of the notation used here and of the steps for calculating the asymmetry are provided in Table S3 and Table S4 in the Supplementary Information.

2.2 Relationship between asymmetry and environmental drivers

To investigate the drivers of temporal asymmetry of NEP, we examined the relationship between the maximum asymmetry (A^{max}) and site-averaged environmental conditions including three year and matching averages of Air Temperature (T),

https://doi.org/10.5194/egusphere-2026-3770
Preprint. Discussion started: 7 July 2026

Shortwave Radiation (SW), Soil Moisture (SM), Precipitation (P), Vapor Pressure Deficit (VPD), and the ratio of Mean Annual Temperature to Mean Annual Precipitation (MAT: MAP) for 13 sites spanning 7 biomes (Table S1).

We use the full-record averages (i.e., averaged over the 3 year study period at each site) of environmental drivers as proxies for the potential long-term climatological baselines that shape an ecosystem's structure and physiological capacity over time. Long-term climate regimes influence an ecosystem's maximum photosynthetic thresholds (Duffy et al., 2021; Chaves et al., 2016), canopy architecture (e.g., maximum LAI) (Migliavacca et al., 2021), and physiological strategies (Chaves et al., 2016; Migliavacca et al., 2021). To consider event-level environmental conditions (i.e., environmental variables averaged only over the periods when the selected fluctuations occur), we also use matching averages of all drivers (e.g., average of temperature during selected fluctuations). Matching averages were comparable to the full-record averages in terms of the dominant drivers and correlation strengths (Tables S6 and S7).

For each driver, we considered seven candidate functions widely used in environmental sciences including linear, quadratic, power, exponential, logarithmic, sigmoid, and Hill equations, and selected the best fitting model using multiple objective criteria. Model performance was assessed using the coefficient of determination (R^2), R^2 adjusted, root mean square error (RMSE), Pearson correlation, p-value and information criteria including Akaike Information Criterion (AIC), Corrected Akaike Information Criteria (AICc), and Bayesian Information Criteria (BIC). BIC was used as the primary selection metric because it poses the strongest penalty for additional parameters, while AIC, adjusted R^2, and RMSE served as secondary criteria. Tables S6 and S7 in the Supplementary Information summarize the best fit relationships and the values of all the statistical metrics for all variables for large top 1 % fluctuations and all fluctuations respectively.

3 Results and discussion

Figure 2 illustrates an example of NEP time-series for four selected sites, each with three years of continuous data, along with their corresponding probability density functions (PDFs). The NEP values exhibit continuous variability, typically around ≈ 0, representing the net absorption (NEP> 0) and release (NEP< 0) of CO_2 by ecosystems, driven by photosynthesis and respiration, respectively. The magnitude of NEP peaks varies depending on the biome, with deciduous broadleaf forests showing higher positive and negative peaks driven by higher photosynthetic and respiration rates (i.e., due to their larger canopy and biomass). Additionally, across all the sites analyzed, the positive tails of the PDFs tend to decay more slowly than do the negative tails, suggesting a common trend of more positive than negative fluctuations consistent with net carbon sink behavior (Li et al., 2022). Although the PDFs describe the distributions of the NEP values, they contain no information about the temporal ordering of values within a fluctuation—two ecosystems with PDFs that are identical may demonstrate opposite asymmetries of how NEP increases toward and decreases from its peak. Therefore, the analyses here focuses on the temporal asymmetry of the NEP values, which captures directional information about ecosystem carbon dynamics that cannot be revealed by the distributional characteristics of the NEP values.

https://doi.org/10.5194/egusphere-2026-3770
Preprint. Discussion started: 7 July 2026

3.1 NEP variability and asymmetry across statistically extreme top 1 % fluctuations

When the top 1 % of NEP fluctuations (extremes) are considered (c = 99 % quantile), the daily average fluctuations exhibit positive asymmetry, with the falling limb of the fluctuations decaying more slowly than the rising limb, indicating that afternoons remain more productive—or at least equally productive—as mornings, resulting in positive asymmetry of NEP. As shown in Figure 3(a), fluctuations asymmetry in the top 1 % fluctuations is evident across all sites, irrespective of their specific biomes, The same analysis shown separately for all 13 sites is presented as Figure S2 in the Supplementary Information. Compared to Figure 3(c), the patterns in Figure 3(a) show greater similarity across various biomes, indicating a potential convergent response of ecosystem carbon dynamics under extreme flux conditions. This convergence of NEP trajectories implies that despite biome-specific differences under average conditions, large deviations in NEP tend to follow a common post-peak behavior, potentially reflecting shared physiological constraints.

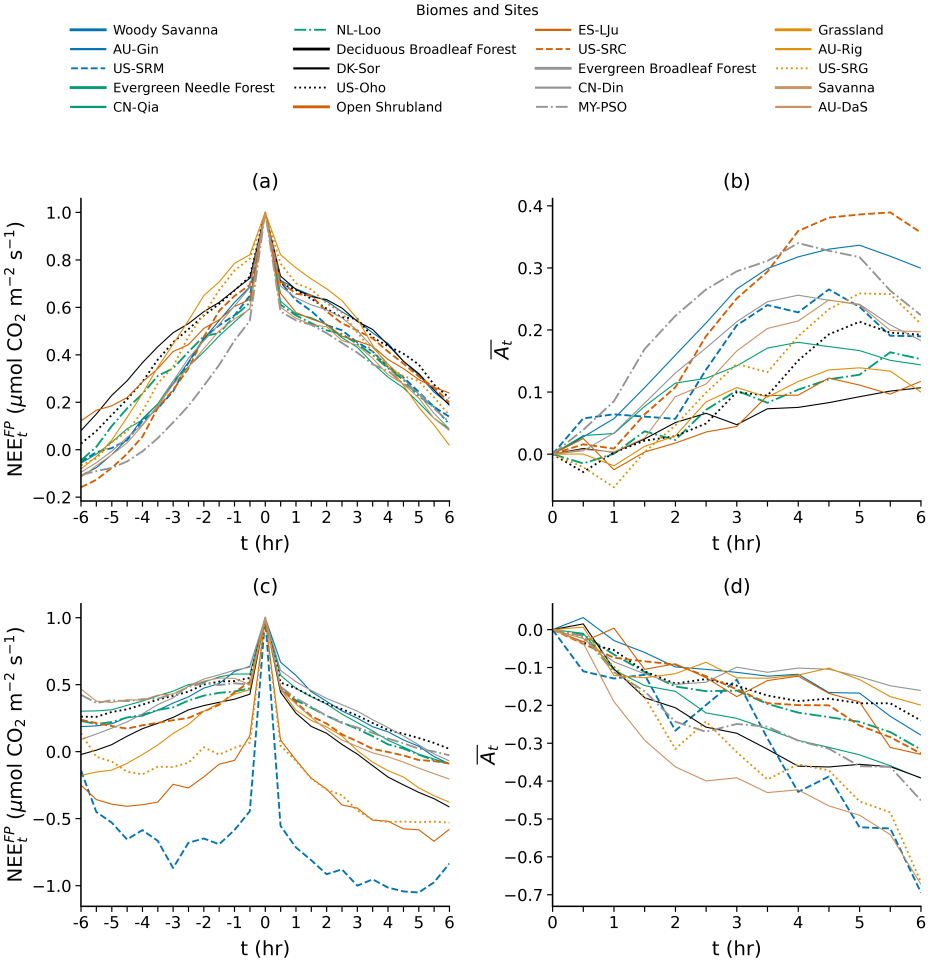

Figure 3. Mean fluctuation paths and asymmetry coefficients for the top 1 % extreme fluctuations and all fluctuations across the 13 study sites. Panels (a) and (b) show top 1 %; panels (c) and (d) show all fluctuations.

https://doi.org/10.5194/egusphere-2026-3770
Preprint. Discussion started: 7 July 2026

A pattern of positive asymmetry is observed for extremes at all sites. As shown in Figure 3(b), the statistical difference between the falling limb and rising limb is captured in the asymmetry coefficient. Initially, at $t = 0$, the asymmetry is zero. However, with increasing t, the asymmetry coefficient gradually increases, ultimately reaches a final plateau (up to $A_t \approx 0.5$). The analysis carried out on all 13 sites separately, see Figure S4 of the Supplementary Information, confirms this overall trend. The trend results from NEP decaying very quickly after reaching its peak (approximately as fast as it reached the peak, hence low asymmetry), and then decaying slowly (slower than the rising limb) far from the peak. This slower relaxation results in higher asymmetries at longer times, as curiously—but hardly accidentally—observed also in purely physical systems (Giberti et al., 2007; Iacobello et al., 2023). The highest asymmetry coefficient value is observed for the open shrubland (US-SRC) site (Figure 3). This elevated asymmetry may arise from enhanced afternoon respiration during warm winter days when soil temperatures increase sufficiently, particularly in sites with exposed soils. Similar asymmetry is observed when analyzing the top 2 % and 5 %, although with a lower magnitude (Figure S6 in Supplementary Information), suggesting a potential change in asymmetry as more typical fluctuations are included.

This ubiquitous behavior in large fluctuations that results in positive asymmetry reflects the interaction between the environmental drivers that promote high photosynthetic uptake (i.e., primarily solar radiation) and the respiratory and regulatory processes (e.g., plant and microbial respiration, declining radiation, and incipient stomatal limitation) that gradually reduce NEP after the peak. For these top 1 % fluctuations, whereby high NEP values are driven by high GPP values, we expect the strength of positive asymmetry to be closely linked to main drivers of the rate of photosynthesis (e.g., air temperature) and how they influence photosynthesis throughout the day, leading to faster morning rise and a slower, more gradual post-peak decline in the afternoon, increasing asymmetry (Iio et al., 2004; Koyama and Takemoto, 2014). For example, lower temperatures limit both photosynthesis and respiration, resulting in relatively balanced rise and fall patterns and lower positive asymmetry, as observed in sites NL-Loo, US-Oho, and ES-Lju. As air temperature increases across sites, GPP increases and dominates over RECO, leading to high NEP peaks associated with larger positive asymmetry (see sites AU-Gin, US-SRC, and CN-Din).

3.2 NEP variability and asymmetry across all fluctuations

When all fluctuations are considered (c = 0), asymmetry shifts markedly to negative values across all sites (Figure3(c,d)), with the falling limb being steeper than the rising limb, indicating that NEP is skewed toward the morning, when photosynthetic uptake dominates. While the interaction between environmental drivers and ecosystem response can be unique to each site due to factors such as climate, vegetation type, location, and topography, interestingly a similar pattern of negative asymmetry is observed across sites with values as low as -0.7 (Figure3(d)). This analysis is repeated for each site separately, see Figure S3 and Figure S5 in Supplementary Information. NEP increases gradually in the morning, driven by photosynthesis. Towards midday, GPP decreases rapidly, while respiration remains more steady, causing steep afternoon NEP declines and negative asymmetry (Novick et al., 2016; Grossiord et al., 2020). This pattern is suggestive of a photosynthesis-driven decline combined with continued respiration.

While asymmetry is negative across sites, the level of asymmetry varies by biome and site-specific aspects of the biomes, with the asymmetry coefficients generally found between –0.10 and –0.70. The Savanna ecosystem (AU-DaS) has the highest

https://doi.org/10.5194/egusphere-2026-3770
Preprint. Discussion started: 7 July 2026

negative asymmetry coefficient, while the evergreen forest ecosystems (MY-PSO, CN-Qia) and the grassland site (AU-Rig) have moderate to smaller negative asymmetry coefficients. These spatial differences observed in asymmetry further suggest a possible relation to site-level variation in evaporative demand. Ecosystems such as savannas with low soil moisture which experience higher afternoon VPD and stronger stomatal limitation, exhibit more negative asymmetry, whereas ecosystems with lower VPD exposure such as evergreen forests and grasslands show weaker asymmetry (Zhang et al., 2023; Chaves et al., 2016).

3.3 Linking asymmetry to environmental drivers and physiological mechanisms

To help interpret these patterns in asymmetry, it is useful to analyze the correlation of the maximum in asymmetry coefficients to environmental drivers (see Figures S7 to S17 in the Supplementary Information), an analysis that can further support the regime-dependent nature of asymmetry across sites.

For the top 1 % fluctuations, $A^{\max}$ shows a strong relationship with mean air temperature, best described by a Hill function. The Hill's equation yielded the lowest BIC value of –61.79, the highest adjusted R^2 of 0.5089, and RMSE = 0.0762. We find that the peak in asymmetry, $A^{\max}$, follows an increasing trend with the average air temperature of the sites during the studied period (Figure 4(a)). The curve rises sharply to a maximum of ≈ 0.45 between 10°C–22°C, before plateauing at the sites with higher temperatures. This pattern reflects the physiological basis of statistical extremes, where higher temperatures amplify photosynthesis (GPP), resulting in increased asymmetry produced from larger differences between the rising and falling limbs. As sites continue to experience increases in mean temperature and it becomes high enough for GPP to approach its physiological limit, the differential response between GPP and RECO saturates, causing asymmetry to plateau around 0.45 (Duffy et al., 2021; Yang et al., 2021). In contrast, sites with lower temperatures display lower $A^{\max}$, where the rising and falling limbs show lower positive asymmetry. Compared to mean air temperature, other environmental variables showed only secondary associations with asymmetry. Shortwave radiation has a positive correlation with asymmetry ($r = 0.53$ for 3-year average and $r = 0.41$ for daily average, Table S6 and Fig. S7 in SI), reflecting its role in steep morning NEP rises. VPD also exerts a modest positive correlation in this regime ($r \approx 0.44$–0.49, p=0.09–0.13, Table S6 and Fig. S10 in SI), reinforcing positive asymmetry when coupled with high radiation, while soil moisture and precipitation show weak to very weak correlations (Figs. S8–S9 in SI). The 3-year T:P ratio exhibits a weak positive correlation ($r \approx 0.30$, p=0.31, Table S6 and Fig. S11 in SI), suggesting that ecosystems with stronger forcing relative to precipitation tend to sustain higher positive asymmetry in extreme fluctuations.

https://doi.org/10.5194/egusphere-2026-3770
Preprint. Discussion started: 7 July 2026

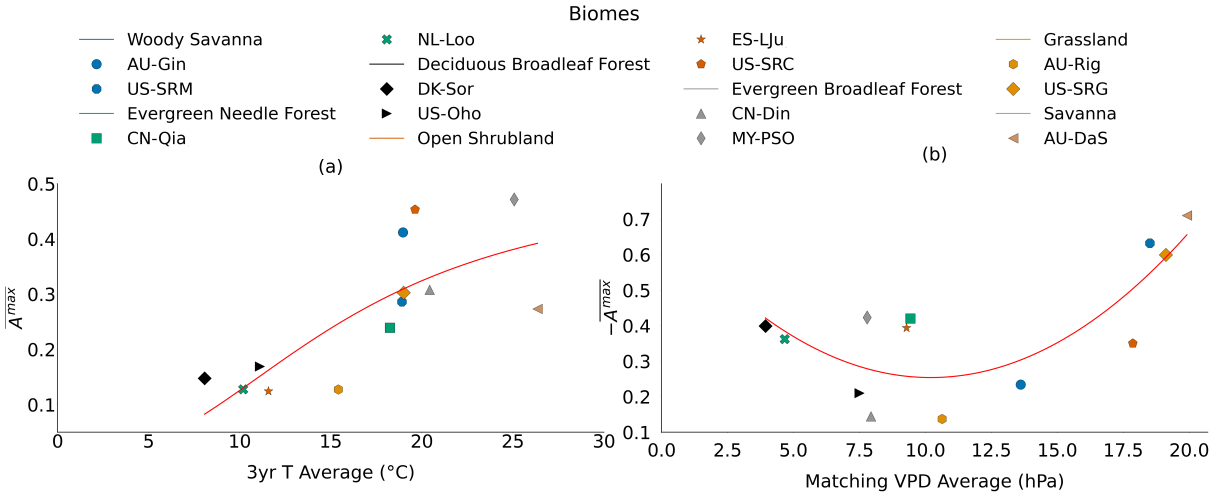

Figure 4. Relationship between $\overline{A^{max}}$ and (a) 3-year average temperature for the top 1 % fluctuations ($c = 99\,\%$ quantile) and (b) matching average VPD for all fluctuations. The red curves represent the best-fit model for each scenario: a hill function for temperature (panel a) and a quadratic function for VPD (panel b). Statistical metrics for each fit are reported in the legend boxes, including R^2, adjusted R^2, RMSE, AIC, AICc, BIC, Pearson correlation, and p-value.

For all fluctuations, asymmetry shows the strongest negative correlation with mean VPD ($r = -0.59$ across scales; Figure 4(b) and Figure S17). A quadratic fit best captures this relationship (with the lowest BIC of -50.98, the highest adjusted R^2 of 0.5136, and RMSE $= 0.1047$), demonstrating the non-linear variation in asymmetry with increasing evaporative demand. At low to intermediate VPD (4–12 hPa), asymmetry is moderately negative ($A^{\max} \approx -0.2$ to -0.4), implying that the morning rise and afternoon decline are comparatively well balanced. As mean VPD increases across sites (generally driven by high values in the afternoon), stomata close in order to conserve water, causing a rapid drop in photosynthesis while respiration continues, resulting in a steep NEP decline (Novick et al., 2016). This leads to a strong negative asymmetry at high VPD (e.g., $A^{\max} < -0.6$ for VPD > 18 hPa). In addition to VPD, temperature also shows a negative correlation ($r = -0.34$ for daily average and $r = -0.38$ for 3-year average, p=0.20-0.25, Table S7 and Fig. S12 in SI). Soil moisture shows a positive correlation across sites ($r \approx 0.32$ across both daily and 3-year scales, p=0.28–0.29, Table S7 and Fig. S14 in SI), reflecting differences in the levels of water availability that influence stomatal opening, while shortwave radiation correlates negatively with asymmetry (Fig. S13 in SI) and precipitation exhibits weak or negligible effects (Table S7 in SI). The T:P ratio also shows a weak negative correlation in this regime ($r = -0.2$, Table S7 and Fig. S16 in SI).

3.4 Regime-dependent asymmetry

A central finding of this study is the regime-dependent flip in the sign of asymmetry, contrasting typical daily fluctuations with statistically extreme events (see Figures 3a-3d), and marking a shift in the dominant controls of ecosystem carbon dynamics. As evident in Figure 5, for extremes (c = 99 % quantile), the peak asymmetry is positive, whereby NEP rises rapidly in the morning as photosynthesis increases, reaching a midday peak, and then declines more gradually in the afternoon. For all fluctuations (c=0), the peak asymmetry is negative, whereby NEP rises gradually in the morning and then declines rapidly in the afternoon,

https://doi.org/10.5194/egusphere-2026-3770
Preprint. Discussion started: 7 July 2026

reflecting stronger attenuation of photosynthesis in the afternoon, producing a steeper falling limb. These differing responses between extremes and typical daily peaks are due to differences in the timing of how photosynthesis and respiration respond to daily changes in the environmental drivers. This systematic flip across all 13 sites, regardless of biome type, can also be observed from the behavior of the average asymmetry coefficient (not just the maximum) illustrated in Figure S6.

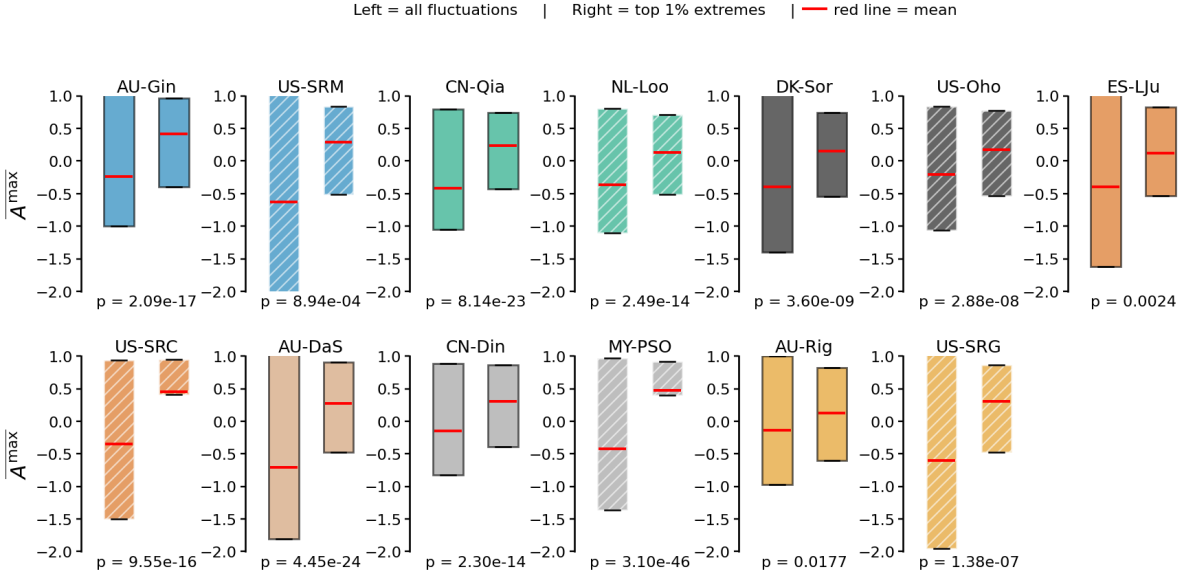

Figure 5. Comparison of peak values $\overline{A^{max}}$ for all fluctuations (left) and the top 1 % extremes fluctuations (right) across sites. Red lines indicate the mean values. P-values from Welch's t-test are reported beneath each panel.

From an ecosystem perspective, the findings show that during large NEP fluctuations, asymmetry is controlled by temperature: higher temperatures enhance photosynthetic capacity, producing an accelerated morning GPP rise followed by a slower afternoon decline, leading to positive asymmetry (Duffy et al., 2021; Yang et al., 2021) (Fig. 4(a)). By contrast, the asymmetry of the average diurnal cycle (i.e., all fluctuations) is primarily controlled by VPD, as high evaporative demand triggers rapid stomatal closure and a steep afternoon GPP decline while RECO remains more steady, contributing to negative asymmetry (Chaves et al., 2016) (Fig. 4(b)).

This universal flip highlights the fact that ecosystems can operate under two fundamentally different dynamical regimes based on the amplitude of NEP fluctuations, one in which NEP is governed primarily by changes in GPP (linked to temperature) and another in which RECO plays a larger role, although GPP decline (dominated by VPD-driven stomatal closure) — still modulates the NEP decline. Similar switching between GPP- or RECO-controlled NEP has also been observed in diurnal cycles across seasons (Räsänen et al., 2017) or in inter-annual variability across vegetation types (Yuan et al., 2009). Although our analysis quantifies asymmetry for the integrated NEP flux rather than for GPP and RECO individually, the regime-dependent patterns observed here are consistent with well-documented physiological mechanisms: VPD-driven afternoon stomatal closure that reduces GPP under typical conditions (Novick et al., 2016; Grossiord et al., 2020), and temperature-regulated photosynthetic capacity that sustains GPP under near-optimal conditions (Duffy et al., 2021; Yang et al., 2021).

https://doi.org/10.5194/egusphere-2026-3770
Preprint. Discussion started: 7 July 2026

The positive asymmetry observed under extreme NEP fluctuations has a direct physiological basis rooted in the same environmental factors that produce these extremes. Reaching the top $1\,\%$ of NEP values requires that GPP substantially exceeds RECO throughout the day, which in turn simultaneously requires near optimal environmental conditions for carbon uptake (Chaves et al., 2016; Li et al., 2022). Under such conditions, afternoon stomatal limitation is reduced because VPD is less likely to reach levels that trigger strong stomatal closure (Grossiord et al., 2020), allowing GPP to remain elevated later into the day and producing a more gradual decline after the daily peak. On typical days, by contrast, the full distribution of fluctuations includes many cases when afternoon evaporative demand is higher and photosynthesis is more strongly constrained, leading to a steeper post-peak decline. Therefore, the top $1\,\%$ of NEP values is not an arbitrary cut-off based solely on statistics; rather, it represents conditions characterized by near-optimal carbon assimilation, in contrast to the broader range of conditions in the full distribution, which include varying degrees of physiological limitation in the afternoon. Furthermore, the asymmetry measure provides an objective quantification of both the magnitude and consistency of this regime across different biomes and is complementary to other site-based ecophysiological measures.

For top 1 % fluctuations, $A^{\max}$ distributions are predominantly positive across all sites, indicating that the observed positive asymmetry reflects a consistent directional difference between the rising and falling limbs rather than arising from cancellation artifacts (Fig. 5). For all fluctuations, $A^{\max}$ distributions are predominantly negative across most sites, although a small number of sites exhibit broader distributions spanning both signs. This indicates site-level variability in the strength of afternoon NEP suppression, rather than systematic cancellation effects.

3.5 Outliers and biome-specific deviations

For the top 1 % fluctuations, the AU-DaS site (Savanna) emerges as an outlier, exhibiting lower asymmetry ($\overline{A^{max}} = 0.273$) despite having high mean air temperature ($\sim 27\,^{\circ}\mathrm{C}$), and falling below the fitted curve (Fig. 4(a)). The combination of extremely high 3-year average shortwave radiation ($\sim 235\ \mathrm{W\,m^{-2}}$), high VPD ($\sim 15\ \mathrm{hPa}$), very low soil moisture ($\sim 5\ \mathrm{mm}$), and a low MAT:MAP ratio (~ 300) likely contributes to strong water limitation, restricting stomatal activity and limiting large GPP peaks. This results in a lower-than-expected $\overline{A^{max}}$ despite warm temperatures that would otherwise favor high afternoon GPP (Wankmüller et al., 2024; Grossiord et al., 2020; Quan et al., 2013).

For all fluctuations, the US-SRC site (Open Shrubland) stands out as a high-VPD outlier. Despite higher VPD ($\sim 18\ \mathrm{hPa}$), US-SRC shows weaker negative asymmetry ($\overline{A^{max}} \sim -0.35$) (Fig. 4(b)), likely buffered by warm temperatures ($\sim 20\,^{\circ}\mathrm{C}$), very high shortwave radiation, and moderate soil moisture, resulting in more sustained afternoon assimilation. In the T:P ratio relationships (Fig. S16 in the SI), US-SRC again deviates from expectation, along with AU-DaS (Savanna). Specifically, US-SRC shows weaker asymmetry (~ -0.35) despite a relatively high T:P ratio (~ 600), while AU-DaS displays very strong negative asymmetry (~ -0.71) despite a lower T:P ratio (~ 300), reflecting the overriding influence of extremely high radiation at this site.

While our analysis provides new insights into ecosystem carbon exchange, it has some inherent limitations related to the FLUXNET2015 dataset. The NEE_VUT_REF product used in our study is a continuous time series, generated through combining and standardizing measured and gap filled hourly values of NEE using the ONEFlux pipeline (Pastorello et al., 2020, 2021).

https://doi.org/10.5194/egusphere-2026-3770
Preprint. Discussion started: 7 July 2026

The MDS gap-filling method generates values for missing data based on meteorologically similar periods that are similar to when the measurement was taken. Therefore, values for missing data will generally reflect "typical" or "average" magnitude of fluxes over a few extreme fluxes. If any of these values exceed the top 1 % threshold, they would most likely reduce instead of increase what may appear to be a positive bias due to net uptake. As shown in section 2.1, only 12.4 % of our identified extreme peaks use data that is replaced by gap-filling. This confirms that the positive asymmetry that we observe during top 1 % extreme conditions is fundamentally caused by measured physical responses and not by artifact associated with gap-filling. Although FLUXNET applies consistent quality control across all sites (Pastorello et al., 2020), the modeled estimates of NEE, GPP, and RECO rely on assumptions that may introduce uncertainty, particularly during rare extreme events (Pastorello et al., 2021; Vekuri et al., 2023; Jung et al., 2024).

4 Implications

Our findings of the regime-dependent asymmetry—positive temporal asymmetry under top 1 % extremes (linked to temperature) and negative asymmetry for typical fluctuations (linked to VPD)—suggest that temporal asymmetry is an emergent property resulting from the nonlinear interactions between ecosystem processes (e.g., processes involving plants, soil microorganisms, abiotic drivers, etc.) under non-equilibrium conditions (Marconi et al., 2008; Evans et al., 2008; Caruso et al., 2020; Amadori et al., 2022; Iannella and Rondoni, 2023) (see Figure 6). Application of a statistical physics measure of asymmetry to NEP time-series provided a first systematic quantification of time-asymmetry, with important insights into the dynamics of land-atmosphere C exchanges. This finding has implications for both fundamental understanding and practical modeling of land-atmosphere carbon exchanges.

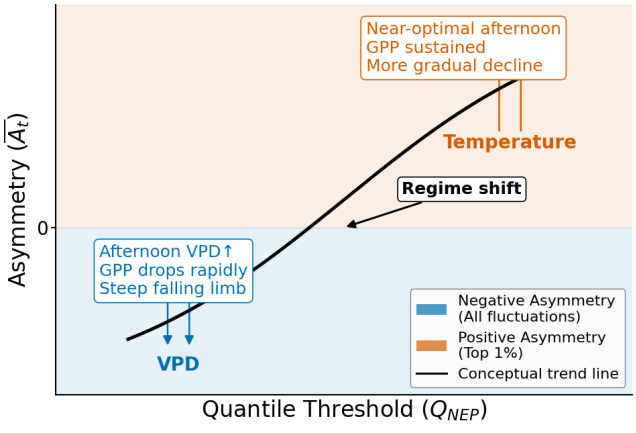

Figure 6. Conceptual schematic of the regime-dependent transition in diurnal NEP temporal asymmetry as a function of the NEP quantile threshold (Q_{NEP}). Negative asymmetry under typical conditions ($c = 0$) is associated with VPD-driven afternoon GPP suppression, while positive asymmetry under extreme fluctuations (top 1 %; $c =$ 99th quantile) occurs when near-optimal afternoon conditions sustain GPP. The dominant control shifts from VPD under typical conditions to temperature under extremes. The black curve represents a conceptual transition between asymmetry regimes.

https://doi.org/10.5194/egusphere-2026-3770
Preprint. Discussion started: 7 July 2026

While a complete characterization of ecosystem non-equilibrium dynamics, à la De Groot and Mazur (De Groot and Mazur, 2013), remains beyond reach, the use of a statistical physics measure allowed an investigation of emergent asymmetric behaviors. In fact, nonequilibrium systems often display convergent behaviors, at least statistically, despite significant spatiotemporal variability (i.e., in NEP). Furthermore, the time-asymmetry quantified here could also be interpreted as a quantification of the average daily hysteresis in the NEP-time space Niu et al. (2011). In particular, the integral of the asymmetry coefficient with respect to τ quantifies the inner area of the average hysteresis loop. The same approach, however, could be used to quantify the hysteresis with respect to environmental drivers Gharari and Razavi (2018). In fact, our measure of time-asymmetry has been more broadly related to system's nonlinear response to external forcing (here environmental forcings driving the C cycle) (Paneni et al., 2008; Caruso et al., 2020) and, thus, could be connected to mathematical biosphere models (Fisher et al., 2014), generally formulated as systems of ODEs, for which a nonlinear response function could be formulated explicitly. While for the asymmetry computed here empirical NEP trajectories are sufficient, in future contributions we will explore this connection between biosphere models and nonlinear response to better elucidate how the asymmetry (and hysteresis) originates from the intrinsic ecosystem's response to environmental drivers and/or the time variability of these same drivers.

An important, practical implication of these findings relates to the development as well as evaluation of predictive models for NEP. Terrestrial biosphere models and machine learning techniques are common approaches to predict NEP based on environmental drivers. These models aim to capture multiple nonlinear interactions in an ecosystem, resulting in very detailed, high dimensional models. These are typically calibrated using long-term time-series data dominated by typical conditions. However, if nonlinear interactions during large fluctuations manifest into peculiar ecosystem behavior (positive asymmetry), suggesting further complexity, it would be informative to calibrate model parameters by appropriately considering these large fluctuations. Incorporating asymmetry and explicitly accounting for regime-dependent dynamics can improve calibration and prediction, particularly for the tails of the NEP distribution that matter most under disturbance or climate extremes. Hence, while simpler models could be suitable for predicting NEP under regular conditions (in line with evidence that ecosystem dynamics is often captured by few key dimensions (Migliavacca et al., 2021)), more complex nonlinear models able to capture extremes may be needed for a complete representation of ecosystem dynamics, including large fluctuations.

Importantly, positive asymmetry typically associated to stronger environmental forcings emerges only during large fluctuations. This emphasizes the importance of studying large fluctuations to better capture nonlinear ecosystem dynamics, critical for understanding ecosystem response to disturbances or extreme events (Lemoine, 2021). This stresses the importance of long-term ecosystem monitoring to capture and harness the information contained in these fluctuations (Turner and Seidl, 2023). From a management perspective, recognizing the role of asymmetry and extremes can help develop strategies for sustaining ecosystem stability and carbon balance under intensifying variability (Weiskopf et al., 2020).

Finally, while here we focused on ecosystems in their stationary state, in future work we will investigate the effects of human and climate disturbances. These include land-use changes, such as deforestation and urbanization, as well as heat waves, fires, and droughts, all of which can profoundly alter soil and vegetation status and their interactions, resulting in significant changes in NEP dynamics. Thermodynamic quantities (e.g., entropy production) have recently been used to evaluate ecosystem conditions, for example to quantify the sustainability of agroecosystems using the entropy production as a proxy (Artuzo et al.,

https://doi.org/10.5194/egusphere-2026-3770
Preprint. Discussion started: 7 July 2026

2021). Similarly, the use of temporal asymmetry (in physical systems related to irreversibility and entropy production) in NEP time-series as a measure of the impact of ecosystem disturbances on ecosystem C dynamics, resilience, and recovery, deserves further investigation.

5 Conclusions

Despite the large spatio-temporal variability observed in NEP time-series, complex systems often exhibit emergent behaviors captured by simple statistical measures. Here, we demonstrated that temporal asymmetry is a key emergent property of ecosystem carbon dynamics that is descriptive of NEP regimes (positive asymmetry for extreme NEP peaks and negative asymmetry for all daily peaks) and their dominant drivers (temperature for positive asymmetry and VPD for negative asymmetry). Considerations of these regimes and their NEP asymmetric behavior adds to our understanding of ecosystem dynamics and provides important insights for advancing process-based and data-driven models.

Code and data availability. Data for this analysis were retrieved from the FLUXNET website (https://fluxnet.org/data/fluxnet2015-dataset/) and is subject to FLUXNET's data use policy. Derived datasets and associated Python code used in this study are available on GitHub (https://github.com/G-NIK-HILA/Time-Asymmetry-of-Ecosystem-Net-Carbon-Exchange), including excel files used for supplementary information, summarizing processed data. This repository will be published in a public repository upon completion of peer review.

Author contributions. **Nikhila Gollakota**: Conceptualization, Data Curation, Formal Analysis, Investigation, Methodology, Writing – original draft, Writing – review & editing.

Salvatore Calabrese: Conceptualization, Methodology, Supervision, Investigation, Funding Acquisition, Writing – review & editing.

Georgianne Moore: Investigation, Methodology, Writing – review & editing.

Lamberto Rondoni: Investigation, Methodology, Writing – review & editing.

Binayak Mohanty: Investigation, Writing – review & editing.

Heng Huang: Investigation, Writing – review & editing.

Competing interests. The authors declare that they have no conflict of interest.

Acknowledgements. The authors acknowledge the Water Management and Hydrologic Science program at Texas A&M University. Any opinions, findings, and conclusions or recommendations expressed in this material are those of the author(s) alone.

https://doi.org/10.5194/egusphere-2026-3770
Preprint. Discussion started: 7 July 2026

Financial support. This work was supported by the USDA National Institute of Food and Agriculture (Hatch projects 1023954, 7010390). This work has been performed under the auspices of Italian National Group of Mathematical Physics (GNFM) of the Istituto Nazionale di Alta Matematica (INdAM). LR acknowledges that this work is part of the project NODES which has received funding from the MUR - M4C2 1.5 of PNRR funded by the European Union - NextGenerationEU (Grant agreement no. ECS00000036).

https://doi.org/10.5194/egusphere-2026-3770
Preprint. Discussion started: 7 July 2026

References

Amadori, D., Colangeli, M., Correa, A., and Rondoni, L.: Exact response theory and Kuramoto dynamics, Physica D: Nonlinear Phenomena, 429, 133 076, 2022.

Andrieux, D., Gaspard, P., Ciliberto, S., Garnier, N., Joubaud, S., and Petrosyan, A.: Entropy production and time asymmetry in nonequilibrium fluctuations, Physical review letters, 98, 150 601, 2007.

Artuzo, F. D., Allegretti, G., Santos, O. I. B., da Silva, L. X., and Talamini, E.: Emergy unsustainability index for agricultural systems assessment: A proposal based on the laws of thermodynamics, Science of the total environment, 759, 143 524, 2021.

Baldocchi, D.: 'Breathing'of the terrestrial biosphere: lessons learned from a global network of carbon dioxide flux measurement systems, Australian Journal of Botany, 56, 1–26, 2008.

Braswell, B. H., Sacks, W. J., Linder, E., and Schimel, D. S.: Estimating diurnal to annual ecosystem parameters by synthesis of a carbon flux model with eddy covariance net ecosystem exchange observations, Global Change Biology, 11, 335–355, 2005.

Caruso, S., Giberti, C., and Rondoni, L.: Dissipation function: Nonequilibrium physics and dynamical systems, Entropy, 22, 835, 2020.

Chaves, M., Costa, J. M., Zarrouk, O., Pinheiro, C., Lopes, C., and Pereira, J. S.: Controlling stomatal aperture in semi-arid regions—The dilemma of saving water or being cool?, Plant Science, 251, 54–64, 2016.

Cochran, F. V., Brunsell, N. A., and Suyker, A. E.: A thermodynamic approach for assessing agroecosystem sustainability, Ecological indicators, 67, 204–214, 2016.

De Groot, S. R. and Mazur, P.: Non-equilibrium thermodynamics, Courier Corporation, 2013.

Dietze, M. C., Vargas, R., Richardson, A. D., Stoy, P. C., Barr, A. G., Anderson, R. S., Arain, M. A., Baker, I. T., Black, T. A., Chen, J. M., et al.: Characterizing the performance of ecosystem models across time scales: A spectral analysis of the North American Carbon Program site-level synthesis, Journal of Geophysical Research: Biogeosciences, 116, 2011.

Duffy, K. A., Schwalm, C. R., Arcus, V. L., Koch, G. W., Liang, L. L., and Schipper, L. A.: How close are we to the temperature tipping point of the terrestrial biosphere?, Science Advances, 7, eaay1052, 2021.

Evans, D. J. and Searles, D. J.: The fluctuation theorem, Advances in Physics, 51, 1529–1585, 2002.

Evans, D. J., Searles, D. J., and Williams, S. R.: On the fluctuation theorem for the dissipation function and its connection with response theory, The Journal of chemical physics, 128, 014 504, 2008.

Fang, X., Kruse, K., Lu, T., and Wang, J.: Nonequilibrium physics in biology, Reviews of Modern Physics, 91, 045 004, 2019.

Fisher, J. B., Huntzinger, D. N., Schwalm, C. R., and Sitch, S.: Modeling the terrestrial biosphere, Annual review of environment and resources, 39, 91–123, 2014.

Gharari, S. and Razavi, S.: A review and synthesis of hysteresis in hydrology and hydrological modeling: Memory, path-dependency, or missing physics?, Journal of hydrology, 566, 500–519, 2018.

Giberti, C., Rondoni, L., and Vernia, C.: Temporal asymmetry of fluctuations in the nonequilibrium FPU model, Physica D: Nonlinear Phenomena, 228, 64–76, 2007.

Grossiord, C., Buckley, T. N., Cernusak, L. A., Novick, K. A., Poulter, B., Siegwolf, R. T., Sperry, J. S., and McDowell, N. G.: Plant responses to rising vapor pressure deficit, New phytologist, 226, 1550–1566, 2020.

Hollinger, D. and Richardson, A.: Uncertainty in eddy covariance measurements and its application to physiological models, Tree physiology, 25, 873–885, 2005.

https://doi.org/10.5194/egusphere-2026-3770
Preprint. Discussion started: 7 July 2026

Huang, H., Calabrese, S., and Rodriguez-Iturbe, I.: Variability of ecosystem carbon source from microbial respiration is controlled by rainfall dynamics, Proceedings of the National Academy of Sciences, 118, e2115283 118, 2021.

Iacobello, G., Chowdhuri, S., Ridolfi, L., Rondoni, L., and Scarsoglio, S.: Coherent structures at the origin of time irreversibility in wall turbulence, Communications Physics, 6, 1–8, 2023.

Iannella, L. and Rondoni, L.: Exact Response Theory for Time-Dependent and Stochastic Perturbations, Entropy, 26, 12, 2023.

Iio, A., Fukasawa, H., Nose, Y., and Kakubari, Y.: Stomatal closure induced by high vapor pressure deficit limited midday photosynthesis at the canopy top of Fagus crenata Blume on Naeba mountain in Japan, Trees, 18, 510–517, 2004.

Jørgensen, S. E. and Svirezhev, Y. M.: Towards a thermodynamic theory for ecological systems, Elsevier, 2004.

Jung, M., Schwalm, C., Migliavacca, M., Walther, S., Camps-Valls, G., Koirala, S., Anthoni, P., Besnard, S., Bodesheim, P., Carvalhais, N., et al.: Scaling carbon fluxes from eddy covariance sites to globe: synthesis and evaluation of the FLUXCOM approach, Biogeosciences, 17, 1343–1365, 2020.

Jung, M., Nelson, J., Migliavacca, M., El-Madany, T., Papale, D., Reichstein, M., Walther, S., and Wutzler, T.: Flagging inconsistencies in flux tower data, Biogeosciences, 21, 1827–1846, 2024.

Keenan, T. and Williams, C.: The terrestrial carbon sink, Annual Review of Environment and Resources, 43, 219–243, 2018.

Keenan, T., Baker, I., Barr, A., Ciais, P., Davis, K., Dietze, M., Dragoni, D., Gough, C. M., Grant, R., Hollinger, D., et al.: Terrestrial biosphere model performance for inter-annual variability of land-atmosphere CO2 exchange, Global Change Biology, 18, 1971–1987, 2012.

Kleidon, A.: Life, hierarchy, and the thermodynamic machinery of planet Earth, Physics of life reviews, 7, 424–460, 2010.

Kleidon, A.: Thermodynamic foundations of the Earth system, Cambridge University Press, 2016.

Koyama, K. and Takemoto, S.: Morning reduction of photosynthetic capacity before midday depression, Scientific Reports, 4, 4389, 2014.

Lasslop, G., Reichstein, M., Papale, D., Richardson, A. D., Arneth, A., Barr, A., Stoy, P., and Wohlfahrt, G.: Separation of net ecosystem exchange into assimilation and respiration using a light response curve approach: critical issues and global evaluation, Global change biology, 16, 187–208, 2010.

Lemoine, N. P.: Unifying ecosystem responses to disturbance into a single statistical framework, Oikos, 130, 408–421, 2021.

Li, J., Kug, J.-S., Park, S.-w., Zhai, P., Huang, M., and Kim, J.-S.: Distinct magnitude asymmetries of daily extreme anomalies in gross primary productivity between forests and non-forests, Climate Dynamics, 59, 767–784, 2022.

Li, S.-G., Asanuma, J., Eugster, W., Kotani, A., Liu, J.-J., Urano, T., Oikawa, T., Davaa, G., Oyunbaatar, D., and Sugita, M.: Net ecosystem carbon dioxide exchange over grazed steppe in central Mongolia, Global Change Biology, 11, 1941–1955, 2005.

Lian, Y., Li, H., Renyang, Q., Liu, L., Dong, J., Liu, X., Qu, Z., Lee, L.-C., Chen, L., Wang, D., et al.: Mapping the net ecosystem exchange of CO2 of global terrestrial systems, International Journal of Applied Earth Observation and Geoinformation, 116, 103 176, 2023.

Marconi, U. M. B., Puglisi, A., Rondoni, L., and Vulpiani, A.: Fluctuation–dissipation: response theory in statistical physics, Physics reports, 461, 111–195, 2008.

Migliavacca, M., Musavi, T., Mahecha, M. D., Nelson, J. A., Knauer, J., Baldocchi, D. D., Perez-Priego, O., Christiansen, R., Peters, J., Anderson, K., et al.: The three major axes of terrestrial ecosystem function, Nature, 598, 468–472, 2021.

Niu, S., Luo, Y., Fei, S., Montagnani, L., Bohrer, G., Janssens, I. A., Gielen, B., Rambal, S., Moors, E., and Matteucci, G.: Seasonal hysteresis of net ecosystem exchange in response to temperature change: patterns and causes, Global Change Biology, 17, 3102–3114, 2011.

Novick, K. A., Ficklin, D. L., Stoy, P. C., Williams, C. A., Bohrer, G., Oishi, A. C., Papuga, S. A., Blanken, P. D., Noormets, A., Sulman, B. N., et al.: The increasing importance of atmospheric demand for ecosystem water and carbon fluxes, Nature climate change, 6, 1023–1027, 2016.

https://doi.org/10.5194/egusphere-2026-3770
Preprint. Discussion started: 7 July 2026

Paneni, C., Searles, D. J., and Rondoni, L.: Temporal asymmetry of fluctuations in nonequilibrium steady states, The Journal of chemical physics, 124, 114 109, 2006.

Paneni, C., Searles, D. J., and Rondoni, L.: Temporal asymmetry of fluctuations in nonequilibrium steady states: Links with correlation functions and nonlinear response, The Journal of chemical physics, 128, 164 515, 2008.

Pastorello, G., Trotta, C., Canfora, E., Chu, H., Christianson, D., Cheah, Y.-W., Poindexter, C., Chen, J., Elbashandy, A., Humphrey, M., et al.: The FLUXNET2015 dataset and the ONEFlux processing pipeline for eddy covariance data, Scientific data, 7, 225, 2020.

Pastorello, G., Trotta, C., Canfora, E., Chu, H., Christianson, D., Cheah, Y.-W., Poindexter, C., Chen, J., Elbashandy, A., Humphrey, M., et al.: Author Correction: The FLUXNET2015 dataset and the ONEFlux processing pipeline for eddy covariance data, Scientific data, 8, 72, 2021.

Ping, J., Cui, E., Du, Y., Wei, N., Zhou, J., Wang, J., Niu, S., Luo, Y., and Xia, J.: Enhanced causal effect of ecosystem photosynthesis on respiration during heatwaves, Science Advances, 9, eadi6395, 2023.

Porporato, A., Kramer, P., Cassiani, M., Daly, E., and Mattingly, J.: Local kinetic interpretation of entropy production through reversed diffusion, Physical Review E, 84, 041 142, 2011.

Quan, C., Han, S., Utescher, T., Zhang, C., and Liu, Y.-S. C.: Validation of temperature–precipitation based aridity index: Paleoclimatic implications, Palaeogeography, Palaeoclimatology, Palaeoecology, 386, 86–95, 2013.

Räsänen, M., Aurela, M., Vakkari, V., Beukes, J. P., Tuovinen, J.-P., Van Zyl, P. G., Josipovic, M., Venter, A. D., Jaars, K., Siebert, S. J., et al.: Carbon balance of a grazed savanna grassland ecosystem in South Africa, Biogeosciences, 14, 1039–1054, 2017.

Rastetter, E. B., Griffin, K. L., Kwiatkowski, B. L., and Kling, G. W.: Ecosystem feedbacks constrain the effect of day-to-day weather variability on land–atmosphere carbon exchange, Global Change Biology, 29, 6093–6105, 2023.

Reichstein, M., Falge, E., Baldocchi, D., Papale, D., Aubinet, M., Berbigier, P., Bernhofer, C., Buchmann, N., Gilmanov, T., Granier, A., et al.: On the separation of net ecosystem exchange into assimilation and ecosystem respiration: review and improved algorithm, Global change biology, 11, 1424–1439, 2005.

Reitz, O., Graf, A., Schmidt, M., Ketzler, G., and Leuchner, M.: Upscaling net ecosystem exchange over heterogeneous landscapes with machine learning, Journal of Geophysical Research: Biogeosciences, 126, e2020JG005 814, 2021.

Rondoni, L.: Introduction to nonequilibrium statistical physics and its foundations, Frontiers and Progress of Current Soft Matter Research, pp. 1–82, 2021.

Schimel, D., Schneider, F. D., Carbon, J., and Participants, E.: Flux towers in the sky: global ecology from space, New Phytologist, 224, 570–584, 2019.

Stoy, P. C., Katul, G. G., Siqueira, M. B., Juang, J.-Y., McCarthy, H. R., Kim, H.-S., Oishi, A. C., and Oren, R.: Variability in net ecosystem exchange from hourly to inter-annual time scales at adjacent pine and hardwood forests: a wavelet analysis, Tree Physiology, 25, 887–902, 2005.

Stoy, P. C., Richardson, A. D., Baldocchi, D. D., Katul, G. G., Stanovick, J., Mahecha, M. D., Reichstein, M., Detto, M., Law, B. E., Wohlfahrt, G., et al.: Biosphere-atmosphere exchange of CO 2 in relation to climate: a cross-biome analysis across multiple time scales, Biogeosciences, 6, 2297–2312, 2009.

Talkner, P. and Hänggi, P.: Colloquium: Statistical mechanics and thermodynamics at strong coupling: Quantum and classical, Reviews of Modern Physics, 92, 041 002, 2020.

Teng, D., Gong, X., He, X., Wang, J., Lv, G., Wang, J., and Yang, X.: Impact of meteorological variability on diurnal and seasonal net ecosystem productivity in a desert riparian forest ecosystem, Frontiers in Plant Science, 15, 1332 192, 2024.

https://doi.org/10.5194/egusphere-2026-3770
Preprint. Discussion started: 7 July 2026

Toussaint, O. and Schneider, E. D.: The thermodynamics and evolution of complexity in biological systems, Comparative Biochemistry and Physiology Part A: Molecular & Integrative Physiology, 120, 3–9, 1998.

Turner, M. G. and Seidl, R.: Novel disturbance regimes and ecological responses, Annual Review of Ecology, Evolution, and Systematics, 54, 63–83, 2023.

Vargas, R., Detto, M., Baldocchi, D. D., and Allen, M. F.: Multiscale analysis of temporal variability of soil CO2 production as influenced by weather and vegetation, Global Change Biology, 16, 1589–1605, 2010.

Vekuri, H., Tuovinen, J.-P., Kulmala, L., Papale, D., Kolari, P., Aurela, M., Laurila, T., Liski, J., and Lohila, A.: A widely-used eddy covariance gap-filling method creates systematic bias in carbon balance estimates, Scientific Reports, 13, 1720, 2023.

Wankmüller, F. J., Delval, L., Lehmann, P., Baur, M. J., Cecere, A., Wolf, S., Or, D., Javaux, M., and Carminati, A.: Global influence of soil texture on ecosystem water limitation, Nature, 635, 631–638, 2024.

Wehr, R., Munger, J., McManus, J., Nelson, D., Zahniser, M., Davidson, E., Wofsy, S., and Saleska, S.: Seasonality of temperate forest photosynthesis and daytime respiration, Nature, 534, 680–683, 2016.

Weiskopf, S. R., Rubenstein, M. A., Crozier, L. G., Gaichas, S., Griffis, R., Halofsky, J. E., Hyde, K. J., Morelli, T. L., Morisette, J. T., Muñoz, R. C., et al.: Climate change effects on biodiversity, ecosystems, ecosystem services, and natural resource management in the United States, Science of the Total Environment, 733, 137 782, 2020.

Xiao, J., Fisher, J. B., Hashimoto, H., Ichii, K., and Parazoo, N. C.: Emerging satellite observations for diurnal cycling of ecosystem processes, Nature Plants, 7, 877–887, 2021.

Yang, D., Xu, X., Xiao, F., Xu, C., Luo, W., and Tao, L.: Improving modeling of ecosystem gross primary productivity through re-optimizing temperature restrictions on photosynthesis, Science of the Total Environment, 788, 147 805, 2021.

Yin, J., Porporato, A., and Rondoni, L.: Nonequilibrium fluctuations of global warming, Journal of Climate, 37, 2809–2819, 2024.

Yuan, W., Luo, Y., Richardson, A. D., Oren, R., Luyssaert, S., Janssens, I. A., Ceulemans, R., Zhou, X., Grünwald, T., Aubinet, M., et al.: Latitudinal patterns of magnitude and interannual variability in net ecosystem exchange regulated by biological and environmental variables, Global change biology, 15, 2905–2920, 2009.

Zhang, Z., Cescatti, A., Wang, Y.-P., Gentine, P., Xiao, J., Guanter, L., Huete, A. R., Wu, J., Chen, J. M., Ju, W., et al.: Large diurnal compensatory effects mitigate the response of Amazonian forests to atmospheric warming and drying, Science advances, 9, eabq4974, 2023.